Psychiatry Research: Neuroimaging 232 (2015) 106–114

Contents lists available at ScienceDirect

Psychiatry Research: Neuroimaging

journal homepage: www.elsevier.com/locate/psychresns

Disrupted fornix integrity in children with chromosome 22q11.2 deletion syndrome

Yi Deng [a,b], Naomi J. Goodrich-Hunsaker [a,b], Margarita Cabaral [a,b], David G. Amaral [a,b], Michael H. Buonocore [c], Danielle Harvey [d], Kristopher Kalish [e], Owen T. Carmichael [e,f], Cynthia M. Schumann [a,b], Aaron Lee [a,b], Robert F. Dougherty [g], Lee M. Perry [g], Brian A. Wandell [g], Tony J. Simon [a,b,*]

[a] Department of Psychiatry and Behavioral Sciences, University of California, Davis, Sacramento, CA 95817, USA
[b] The MIND Institute, University of California, Davis, Sacramento, CA 95817, USA
[c] Department of Radiology, School of Medicine, University of California, Davis, Sacramento, CA 95817, USA
[d] Division of Biostatistics, Department of Public Health Sciences, University of California, Davis, CA 95616, USA
[e] Graduate Group in Computer Science, University of California, Davis, CA 95616, USA
[f] Department of Neurology, School of Medicine, University of California, Davis, Sacramento, CA 95817, USA
[g] Department of Psychology, Stanford University, Stanford, CA 94305, USA

ARTICLE INFO

Article history:
Received 17 April 2014
Received in revised form
30 September 2014
Accepted 4 February 2015
Available online 11 February 2015

Keywords:
Chromosome 22q11.2 deletion
Connectivity
Hippocampal formation
Tractography
Velo-cardio-facial Syndrome

ABSTRACT

The fornix is the primary subcortical output fiber system of the hippocampal formation. In children with 22q11.2 deletion syndrome (22q11.2DS), hippocampal volume reduction has been commonly reported, but few studies as yet have evaluated the integrity of the fornix. Therefore, we investigated the fornix of 45 school-aged children with 22q11.2DS and 38 matched typically developing (TD) children. Probabilistic diffusion tensor imaging (DTI) tractography was used to reconstruct the body of the fornix in each child's brain native space. Compared with children, significantly lower fractional anisotropy (FA) and higher radial diffusivity (RD) was observed bilaterally in the body of the fornix in children with 22q11.2DS. Irregularities were especially prominent in the posterior aspect of the fornix where it emerges from the hippocampus. Smaller volumes of the hippocampal formations were also found in the 22q11.2DS group. The reduced hippocampal volumes were correlated with lower fornix FA and higher fornix RD in the right hemisphere. Our findings provide neuroanatomical evidence of disrupted hippocampal connectivity in children with 22q11.2DS, which may help to further understand the biological basis of spatial impairments, affective regulation, and other factors related to the ultra-high risk for schizophrenia in this population.

1. Introduction

Chromosome 22q11.2 deletion syndrome (22q11.2DS), also known as DiGeorge syndrome (Kirkpatrick and DiGeorge, 1968) and velocardiofacial syndrome (Shprintzen et al., 1978; Shprintzen, 2008), results from a microdeletion within chromosome 22 at band q11.2 (Carey et al., 1992; Driscoll et al., 1992). The prevalence of the 22q11.2DS in the general population is one in 2000–4000 live births (Botto et al., 2003; Shprintzen, 2008). Youth with 22q11.2DS have increased risk of schizophrenia, with up to 45% displaying the prodrome (Baker and Skuse, 2005; Stoddard et al., 2010) and up to 30% developing psychotic disorders when they reach adulthood (Bassett and Chow, 1999; Murphy et al., 1999; Arnold et al., 2001; Kates et al., 2011). In children with 22q11.2DS, nonverbal cognitive and behavioral impairments, especially in visuospatial processing and memory, have been consistently reported (Moss et al., 1999; Swillen et al., 1999a, 1999b; Wang et al., 2000; Bearden et al., 2001; Simon et al., 2005a, 2005b, 2008a; Bish et al., 2007; Karayiorgou et al., 2010). Brain-imaging studies report consistent neuroanatomical changes in individuals with 22q11.2DS (for review, see Karayiorgou et al., 2010), including structural alterations (Eliez et al., 2000; Kates et al., 2001, 2004; Bish et al., 2004; Shashi et al., 2004; Simon et al., 2005c; Campbell et al., 2006; Machado et al., 2007; Beaton et al., 2010), reduced cortical thickness (Bearden et al., 2007, 2009) and gyral complexity (Schaer et al., 2006, 2009; Srivastava et al., 2011); altered connectivity in major white matter fiber tracts (Simon et al., 2005c; Machado et al., 2007; Sundram et al., 2010; Radoeva et al., 2012), some of which correlate with functional

* Correspondence to: MIND Institute, University of California, Davis, 2825 50th Street, Sacramento, CA 95817, USA. Tel.: +1 916 703 0407; fax: +1 916 703 0244.
E-mail address: tjsimon@ucdavis.edu (T.J. Simon).

http://dx.doi.org/10.1016/j.pscychresns.2015.02.002
0925-4927/

impairments (Barnea-Goraly et al., 2003, 2005; Simon et al., 2008b; Radoeva et al., 2012). Notably, many of these brain anomalies are in the midline (Simon et al., 2005c; Campbell et al., 2006; Machado et al., 2007; Beaton et al., 2010), and similar patterns of neural alteration are also reported in people with schizophrenia (for review, see Shenton et al., 2001), though their relationship to the actual psychotic symptomatology remains unclear.

The hippocampal formation plays a critical role in the representation of space and memory, and has been shown to modulate emotional processing (Gray and McNaughton, 2000). In typical developing (TD) children, the volume of the hippocampus appears to be positively associated with verbal and full-scale IQ (Schumann et al., 2007). Impairments in the above cognitive domains, and borderline IQ scores are characteristics of children with 22q11.2DS. Reduced hippocampal volume has been consistently reported in this population (Eliez et al., 2000; Kates et al., 2001, 2004, 2006; Simon et al., 2005c; Campbell et al., 2006; Debbané et al., 2006; Deboer et al., 2007) and was significantly correlated with lower verbal IQ (Deboer et al., 2007). Alterations of the hippocampal formation are considered to be a biomarker for schizophrenia and tend to show a similar pattern of functional relationships to that described above (for review, see Shenton et al., 2001).

Despite the important role that the hippocampus plays in core cognitive, affective and behavioral aspects of the 22q11.2DS phenotype, its connectivity to other brain regions has attracted surprisingly little analytical attention. One key tract to consider is the fornix, a bidirectional fiber tract that connects the hippocampal formation (mainly the subiculum) to the septal nuclei and mammillary bodies in the hypothalamus. It also carries a number of afferent fibers to the hippocampal formation from diverse regions including the septal region, the supramammillary region and the locus coeruleus and raphe nuclei. While not likely its primary function, the fornix has been proposed to be involved in affective function, primarily the regulation of anxiety levels and expression of fear-related behaviors in both rodents and humans (Gray and McNaughton, 2000). If this were to be the case, then it would make this circuit particularly relevant to 22q11.2DS given the high levels of anxiety reported and the recently described relationship between anxiety and adaptive functioning (Green et al., 2009; Angkustsiri et al., 2012). Also of considerable relevance is recent evidence demonstrating the modulating role that anxiety plays in attention and executive functioning (Pérez-Edgar and Fox, 2007; Roy et al., 2008; Bishop, 2009; Krug and Carter, 2010; Pérez-Edgar et al., 2011), which are key components of the schizophrenia endophenotype. Similarly, emotional content significantly impacts memory formation (LeDoux, 2000) and thus can further impact affective dysregulation as in the case of atypical fear extinction and generalization as is common in those with elevated levels of anxiety (Lau et al., 2008; Lissek et al., 2008).

To our knowledge, no detailed study of fornix integrity has ever been reported in children with 22q11.2DS. This may be partly due to the difficulty of registering individual brains to a template that is created by the significant but widely varying midline anomalies that are common in this population (Bish et al., 2004; Antshel et al., 2005; Simon et al., 2005c; Campbell et al., 2006; Machado et al., 2007; Beaton et al., 2010; Karayiorgou et al., 2010). Therefore, in this study, we applied probabilistic diffusion tensor imaging (DTI) tractography to each child's high-resolution DT images in their own native brain space, thereby obviating the complexity of whole brain registration. Our goal was to investigate fornix integrity in children with 22q11.2DS and its relationship with the volume of the hippocampal formation. We hypothesized that fornix fiber integrity is reduced in children with 22q11.2DS, when compared with typically developing children. Moreover, this disrupted fornix integrity would correlate with the volume reductions in the hippocampal formation.

2. Methods

2.1. Participants

Forty-five 7- to 14-year-old children with 22q11.2DS and 38 age-, gender-, and handedness-matched TD children were recruited at the MIND Institute at the University of California, Davis. Children with 22q11.2DS were confirmed by fluorescence in situ hybridization (FISH) testing during recruitment. Their demographics and medication history are summarized in Table 1 and the Supplementary material. The study was approved by the University of California Davis Institutional Review Board. All participants gave written informed assents, and parental consents were also obtained.

2.2. MRI acquisition and preprocessing

Before magnetic resonance imaging (MRI) was performed, all participants underwent acclimation and head motion suppression training in a mock MRI scanner. MRI scans were acquired on a 3 T Siemens Trio MRI System (Siemens Healthcare, Erlangen, Germany) running version VA25A SyngoMR operating software with an eight-channel head coil (Invivo Corporation, Gainesville, FL) at the University of California, Davis Imaging Research Center. For each child, head motion was minimized by placing padding around the head and securing a strap across the forehead. High-resolution T1-weighted images were acquired using a 3D magnetization-prepared rapid gradient echo (MPRAGE) pulse sequence, with the following parameters: 192 sagittal slices; slice thickness = 1 mm, echo time (TE) = 4.82 ms, repetition time (TR) = 2170 ms, flip angle = 7°, field of view (FOV) = 256 mm × 256 mm, matrix size = 256 × 256; receiver bandwidth = 140 Hz/Px; echo spacing = 11.1 ms; voxel size = 1.00 × 1.00 × 1.00 mm^3. DTI data were acquired using the Siemens diffusion-weighted spin-echo echo-planar imaging (EPI) pulse sequence (ep2d_diff) with the following parameters: 40 axial slices; slice thickness = 3.0 mm; slice gap = 0.0 mm; TE = 99 ms; TR = 6700 ms; flip angle = 90°, FOV = 220 mm × 220 mm; matrix size = 128 × 80 based on Partial Phase Fourier = 5/8; Receiver Bandwidth = 1502 Hz/Px; EPI factor = 128; echo spacing = 0.84 ms; voxel size = 1.72 × 1.72 × 3.0 mm^3. Diffusion gradients were applied in 12 directions (specified in the sequence by Siemens) with $b = 1000$ s/mm^2.

All DTI preprocessing steps were conducted using the Stanford open-source VISTASOFT package (http://white.stanford.edu/newlm/index.php/Software) running on MATLAB version 2010a (The Mathworks, Inc., Natick, MA, USA). The details are fully described in other publications (Sherbondy et al., 2008a, 2008b; Yeatman et al., 2011, 2012). Briefly, the steps involve removing eddy current distortions and motion artifacts in the diffusion-weighted images using a 14-parameter constrained nonlinear co-registration procedure based on the expected pattern of eddy-current distortions given the phase-encode direction of the acquired data (Rohde et al., 2004). Each diffusion-weighted image was registered to the non-diffusion-weighted ($b = 0$) images using a two-stage coarse-to-fine approach that maximized the normalized mutual information.

T1 images were skull-stripped and horizontally linearly aligned from the anterior commissure to posterior commissure (referred to as AC − PC aligned). After the linear transformation, the AC − PC aligned brains were resampled to 1-mm isotropic voxels using a 7th-order b-spline algorithm based on code from Statistical Parametric Mapping

Table 1
Participant demographics in typically developing (TD) and 22q11.2DS groups.

	TD ($n = 38$) Mean (S.D.)	22q11.2DS ($n = 45$) Mean (S.D.)	Statistics		
			T	d.f.	*p*-Value
Age (in months)	121.2 (27.5)	130 (22.8)	−1.56	72.05	0.12
Gender (M/F)	19/19	22/23	N/A		0.90
Handedness, right handed, *n* (%)	34 (89.5%)	36 (80%)	N/A		0.51
Verbal IQ	115.3 (13.0)	80.1 (12.8)	11.8	68.4	< 0.001
Performance IQ	115.3 (11.1)	76.5 (13.0)	14.1	73.7	< 0.001
Full Scale IQ	116.2 (10.3)	74.0 (12.4)	16.3	74.1	< 0.001

Note: Welch Two-Sample *t*-test or Chi-squared test.

5 software (SPM5; Wellcome Department of Neuroscience, London, UK). The non-diffusion-weighted images were automatically aligned to individual T1 image using a rigid body mutual information algorithm. All raw diffusion images were resampled to 2-mm isotropic voxels by combining the motion correction, eddy-current correction, and anatomical alignment transforms into one omnibus transform and resampling the data using a 7th-order b-spline algorithm based on code from SPM5 (Ashburner and Friston, 2005).

An eddy current intensity correction (Rohde et al., 2004) was applied to the diffusion-weighted images at the resampling stage. The rotation components of the omnibus coordinate transform were applied to the diffusion-weighting gradient directions to preserve their orientation with respect to the resampled diffusion images. The tensors were fit using a robust least squares algorithm (Chang et al., 2005). The eigenvalues ($\lambda 1$, $\lambda 2$, $\lambda 3$) and eigenvectors ($e1$, $e2$, $e3$) were calculated from each diffusion tensor, and the resulting eigenvalues were later used to compute the fractional anisotropy (FA, Basser and Pierpaoli, 1996) and other diffusion scalars.

2.3. Probabilistic tractography

The body of the fornix was reconstructed in each child's native brain space by connecting a pair of anterior-posterior region-of-interest (ROI) seeds using a probabilistic fiber tracking algorithm ConTrack (Sherbondy et al., 2008a), included as part of the Stanford open-source VISTASOFT package (http://white.stanford.edu/newlm/index.php/ConTrack) running on a 120 processor computing cluster. Compared with deterministic algorithms, ConTrack allows more possible pathway orientations for each DTI sample point. Therefore, it is more sensitive to differentiating pathways that travel closely alongside neighboring fibers.

To ensure precise segmentation, ROI seeds were manually defined in each child's native brain space. Two anterior seed ROIs, one in each hemisphere, were drawn medially on the T1 coronal slice around the fornix bundle at the level of the entry point of the pillars into the body of the fornix where the interventricular foramen (or foramin of Monroe) were present (Fig. 1A). The FA-weighted colored maps were used to verify the separate left and right hemisphere ROIs. Two posterior seed ROIs were drawn on the T1 axial slice capturing the exit point of the body into the crus of the fornix in both hemispheres at the level of the inferior border of the splenium of the corpus callosum (Fig. 1B). The fornix ROIs were carefully seeded under the supervision of an expert neuroanatomist (DGA), particularly at the posterior region near the hippocampal area when the fornix runs parallel to the stria terminalis.

Default sampling parameters were used in ConTrack for the probabilistic tracking: only pathways with length less than 240 mm were retained; bending angle for a single step could not exceed 130°; pathways could not step through grey matter regions, and pathways had an endpoint within both ROIs (Yeatman et al., 2011, 2012, Sherbondy et al., 2008b). The algorithm sampled 100,000 pathways between the anterior and posterior ROIs and the pathway step size was set to 1 mm. Then the resulting 100,000 pathways (Fig. 1C) were scored for their anatomical validity using the following parameters: eta=0.175; sigma-sub-c =14; lambda=1 (Sherbondy et al., 2008b). A subset of the top 1000 (1%) scored pathways were selected in QUENCH (Akers, 2006, Fig. 1D). To minimize the non-relevant pathways at each end point, a threshold of maximum 80 mm length was set to the body of the fornix, after considering for its reconstructed anatomical shapes in both TD and 22q11.2DS groups. Individual reconstructions of the 2D and 3D fornix body structures were reviewed by overlaying the tracts on their T1 images.

2.4. Hippocampal volume extraction

Hippocampal volumes were acquired on the T1-weighted images in each child's native brain space using a semi-automated hippocampus segmentation pipeline (Pluta et al., 2009). Details of this hippocampus segmentation method are fully described in other publications (Pluta et al., 2009; Hunsaker and Amaral, 2014).

In brief, the original T1-weighted images were first horizontally AC−PC aligned by using a rigid-body transformation in the Automatic Registration Toolbox (ART) *acpcdetect* module (http://www.nitrc.org/projects/art/). Next, the image signal intensity inhomogeneity caused by non-uniformities in the radio frequency (RF) receiver coils was corrected by the N4 bias field algorithm (Sled et al., 1998; Tustison et al., 2010) implemented in the Advanced Normalization Tools (ANTs; http://www.picsl.upenn.edu/ANTS/).

To acquire hippocampal volumes in the native brain space of our children sample, we adopted the semi-automated pipeline from ANTs (Pluta et al., 2009), diffeomorphically warping a left-right symmetrical 7.5- to 13.5-year-old child brain template (http://www.bic.mni.mcgill.ca/ServicesAtlases/NIHPD-obj1) with fully labeled hippocampus to each child's brain using partial labeling. This means that when anatomical landmarks were properly placed in the hippocampus of each child's native brain space, the template with a fully pre-labeled segmented hippocampus was warped to each of these children brains, to segment the corresponding hippocampus in their native brain space guided by those landmarks. The benefit of this pipeline is that it only requires an expert neuroanatomist (NJG-H) to delineate the structure on a small subset of the entire sample, a task that has traditionally been difficult given the abnormal hippocampus observed in many of the children with 22q11.2DS. After the semi-automatic process, we further refined the segmented hippocampi by using a machine learning based algorithm that corrects systematic errors in the semi-automated segmentations (Automatic Segmentation Tool Adapter; http://www.nitrc.org/projects/segadapter/). The final volume of each hippocampal formations was obtained after this segmentation correction.

To adjust the hippocampal volume, total gray matter volume was also acquired from each child's brain using Atropos, an open source segmentation algorithm distributed as a part of the ANTs (Avants et al., 2011). Similar to the hippocampi segmentation, the same children template (http://www.bic.mni.mcgill.ca/ServicesAtlases/NIHPD-obj1) was diffeomorphically warped to each child's native brain space using a nonlinear normalization to provide a rough template-based brain extraction. After warping, in the native brain space of each child, a whole brain mask and the spatial prior probability maps of three brain tissues (*i.e.* gray matter, white matter and cerebrospinal fluid) were generated by applying the nonlinear warp to the template priors. Then, three-tissue classifications were acquired by implementing the spatial prior probability maps for each child, and the gray matter volume was used to adjust the hippocampal volume.

2.5. Statistical analysis

For the identified reconstructed typical fornix body structure from each hemisphere, the averaged FA, RD, mean diffusivity (MD) and axial diffusivity (AD) were calculated from the entire tracts respectively using the three tensor-eigenvalues. The length of the tracts was also calculated. To compare the diffusivity along the tract, we further divided individual fiber tracts into 1-mm-long segments, respectively, and then extracted the diffusion properties from each segment along the trajectory using a weighted-average approach (Yeatman et al., 2011).

Statistical analyses were conducted in R, version 2.10.1 (R Development Core Team (2011). R: A language and environment for statistical computing (Foundation for Statistical Computing, Vienna, Austria. ISBN 3-900051-07-0, URL http://www.R-project.org) running on a 64-bit Apple Macintosh Pro Intel Quad Core. A p-value < 0.05 was considered statistically significant. Group differences in the fornix averaged diffusion properties and the volumes of the hippocampal formation between children with 22q11.2DS and TD children were assessed using the Welch Two-Sample t-test or Mann-Whitney U-test depending on the data distribution. Within each group, a simple linear regression model was fit for each averaged diffusivity property using age, gender or handedness as independent variables. Assumptions for all models were checked and were met by the data. At each segment along the tract, group differences in FA and RD were compared using Welch Two-Sample t-test and corrected for multiple comparisons using the False Discovery Rate (FDR). Linear regression models were used to assess the correlation between FA, RD and the volumes of hippocampal formation within each group, with age and gender entered as two covariates.

3. Results

3.1. Less organized fornix in the 22q11.2DS group

Averaged FA, MD, AD and RD from the entire body of fornix fiber tracts were measured in all individuals, except for a small subset of children, all with 22q11.2DS ($n=6$ for the left hemisphere, $n=2$ for the right), for whom ConTrack was unable to identify and completely connect a fiber tract even after 100,000 permutations had been attempted. Several likely reasons for these tracking failures are considered in the discussion session. This subset of children with 22q11.2DS did not differ from the rest in age, gender, handedness and IQs. Exclusion of this subset of children with 22q11.2DS did not dramatically affect the demographic group comparison results presented in Table 1 (data not shown). Compared with the TD children, children with 22q11.2DS presented less organized fornix fibers in both hemispheres. Group differences are summarized in Table 2. As a group, children with 22q11.2DS showed significantly lower FA and higher RD in the body of fornix bilaterally compared with TD children. There was no group difference in AD. In the left hemisphere only, mean MD value was higher in the children with 22q11.2DS than in the TD children.

No gender difference was found in any of the averaged FA, MD, AD or RD values bilaterally in either group (Table 3). In TD children, increasing age was associated with higher AD in the left hemisphere, but with increased RD and MD in the right hemisphere (Table 3). None of the diffusivity property values correlated with age in children with 22q11.2DS (all p values > 0.05). Compared with the right-handed TD children ($n=34$), left-handed children in the TD group ($n=4$) had higher FA but lower RD and MD in the left hemisphere, while having significantly higher FA in the right hemisphere. In contrast, left-handed children in the 22q11.2DS group ($n=9$) had higher MD and AD in the

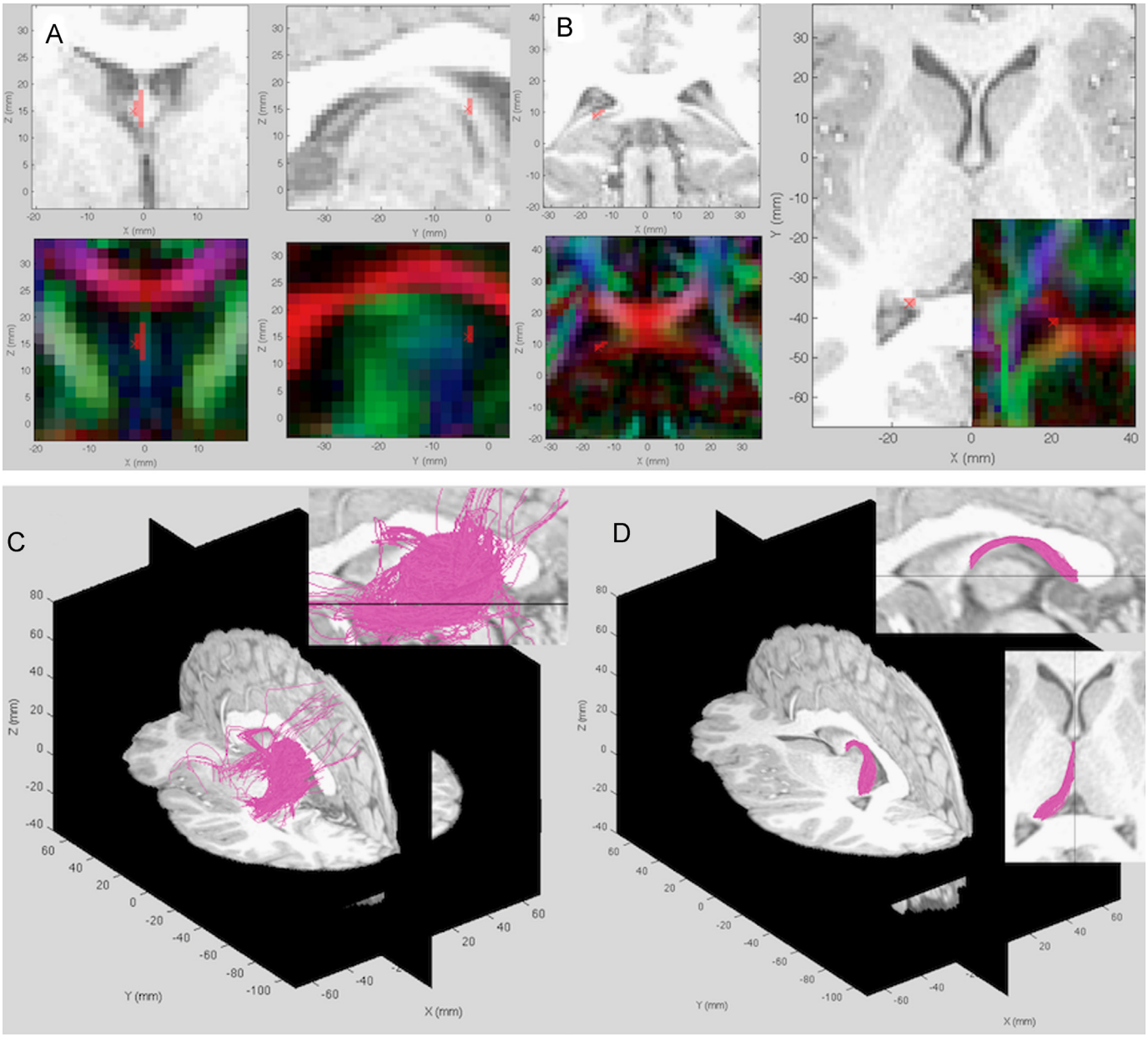

Fig. 1. The method used for identifying the fornix-body tracts in a single participant is illustrated. Estimated tracts on the left side of the brain are shown on the co-registered T1. After manually defining ROIs of anterior (A) and posterior (B) seeds, a set of 100,000 potential pathways connecting two seed points were generated using ConTrack (C). The 1% top scored pathways were selected (D) as a valid subset of pathways.

left hemisphere, in addition to the higher AD in the right hemisphere (Table 3).

3.2. Diffusivity variation along the fornix

We further compared the diffusivity differences along the body of the fornix in segments from the anterior (septal area) to the posterior (caudal hippocampal area). The estimated mean length of the body of the fornix was 45 mm (S.D.= 3 mm) in TD children bilaterally and significantly shorter in children with 22q11.2DS (mean= 39 mm, S.D.= 4mm, $p < 0.001$). Therefore, to perform the along the tract regional comparisons, we divided the fiber tracts of both groups to 45 segments and plotted FA and RD along the trajectory. One child from each group was excluded from the segment analyses in the left hemisphere because the segment diffusion properties could not be extracted due to the limited number of fibers (fewer than 50 out of 1000). Along the trajectory, we found that FA values varied considerably within the tracts, revealing that children with 22q11.2DS had significantly lower FA than TD children in the posterior (steps 24 to 45, $p < 0.05$, FDR corrected) area bilaterally (large gray area in Fig. 2A and B), reflecting the region where fornix fibers depart from the posterior hippocampus. In addition, group differences in FA were also detected at small anterior regions (steps 1 – 3; step 10 – 13 on the left tracts; and step 1 – 5; step 11 – 13 on the right tracts; $p < 0.05$, FDR corrected; small grey area in Fig. 2A and B). In contrast, RD plots showed greater differences on the left body of the fornix, similar to FA (step 1 – 5; 9 – 14 and 24 – 45, $p < 0.05$, FDR corrected, Fig. 2C), but less difference on the right (step 1 – 6 and 42 – 45, respectively, $p < 0.05$, FDR corr;ected, Fig. 2D).

3.3. Correlations between fornix integrity and the volumes of hippocampal formation

As expected, the volumes of the hippocampal formation were found significantly smaller in the 22q11.2DS group than the TD group (Table 4, $t = 6.26$, $p < 0.001$ for left hemisphere; $t = 5.24$, $p < 0.001$ for

right hemisphere, Welch Two-Sample *t*-tests). After controlling for the effect of age and gender, smaller hippocampal formation volumes were correlated with reduced fornix FA and higher fornix RD in the right hemisphere in the 22q11.2DS group but not in the TD group (Table 4 and Fig. 3). Moreover, the correlations were enhanced when we used the fornix FA and RD from the detected significant posterior regions, even though similar correlational patterns were also observed for the detected significant anterior regions (Fig. 3).

4. Discussion

To our knowledge, this is the first DTI tractography study to investigate the fornix integrity in children with 22q11.2DS. Using a probabilistic tracking algorithm ConTrack, we successfully reconstructed the body of the fornix in native brain space of all TD children and most of the children with 22q11.2DS. As a group, children with 22q11.2DS showed significantly lower FA and higher RD values bilaterally in the body of the fornix fiber tracts compared with TD children. Reduced FA and increased RD indicate that the body of the fornix in children with 22q11.2DS may be immature and/or has developed in an atypical fashion. One question of considerable interest in our study was the potential relationship between fornix measurements and the age of the participants. This interest stems from the fact that almost all children with 22q11.2DS suffer from developmental delay to some degree or another. It is not yet clear if this functional delay would be reflected globally, or in specific functional circuits, in the brain. In typically developing children, only axial diffusivity correlated with age in the left hemisphere while radial and mean diffusivity correlated with age in the right hemisphere. These relationships are not easy to interpret in functional terms, but they do suggest that some connectivity changes continue to occur with increasing age in the middle childhood period in typical children. That no such changes could be detected in those children with 22q11.2DS does suggest that similar to other neuroanatomical features (Shashi et al., 2004, 2012; Srivastava et al., 2011; Flahault et al., 2012), there may be a potentially different developmental trajectory in hippocampal connectivity that needs to be explored further.

We further examined FA and RD differences along the entire tract. The tract-based analysis revealed regional integrity differences in children with 22q11.2DS compared with typically developing children. FA reductions in children with 22q11.2DS occurred bilaterally primarily at the posterior body of the fornix, where the fibers projecting from hippocampus run towards the midline. Interestingly, this specific regional FA reduction in children with 22q11.2DS seemed compensated by increasing RD only on the left hemisphere, but not the equivalent area on the right (Fig. 2). The hippocampus is a key structure that is not only involved in memory but that also supports multiple cognitive processes including the representation of space and time (Olsen et al., 2012). Our finding of reduced hippocampal volume in children with 22q11.2DS was in line with recent studies (Kates et al., 2004; Simon et al., 2005c; Campbell et al., 2006; Debbané et al., 2006; Deboer et al., 2007). Given that the fornix is the primary but not limited subcortical efferent projection of the hippocampus, understanding the relationship of fornix integrity to hippocampal anomalies may well enhance our understanding of the neural basis of a range of characteristic cognitive impairments in this population as well as the affective and functional impairments. In studies of aging, reduced fornix FA has been reported as being associated with reduced hippocampal formation volumes, and this degradation of fornix microstructure was found specifically associated with less episodic memory (Metzler-Baddeley et al., 2011; Lee et al., 2012). In this study, we found disrupted fornix integrity, especially from the posterior region, was correlated to the volume reductions of the hippocampal formation exclusively in children with 22q11.2DS. Our findings suggest that there may well be a neuroanatomical foundation for fornix anomalies in the structure of the hippocampus in children with 22q11.2DS. This relationship needs to be further understood and is at the center of our current analyses with a second independent sample of children from the same two populations described here from whom we were able to acquire much higher resolution diffusion weighted as well as structural images with greatly reduced image artifacts.

Another region with FA reductions and RD increases in children with 22q11.2DS was a small section at the rostral extent of the fornix in the subcortical region. The fact that dilated lateral ventricles and/or presence of large cavum septum pellucidum (CSP) was common in these children highlights another relationship worthy of further investigation, namely that between the developmental basis for

Table 2
Average diffusivity properties of the fornix fiber tracts in children with 22q11.2DS and typically developing (TD) children.

	Left			Right		
	TD ($n=38$) Mean (S.D.)	22q11.2DS ($n=39$) Mean (S.D.)	*p*-Value	TD ($n=38$) Mean (S.D.)	22q11.2DS ($n=43$) Mean (S.D.)	*p*-Value
FA	0.37 (0.05)	0.31 (0.06)	< 0.001	0.34 (0.05)	0.29 (0.06)	< 0.001
MD	1.33 (0.10)	1.40 (0.09)	0.003	1.34 (0.09)	1.38 (0.10)	0.068
RD	1.05 (0.12)	1.16 (0.09)	< 0.001	1.08 (0.09)	1.16 (0.09)	< 0.001
AD	1.90 (0.11)	1.89 (0.16)	0.939	1.87 (0.13)	1.83 (0.17)	0.495

Note: Mann – Whitney *U*-test was used for group comparisons.

Table 3
Regression coefficients in a simple linear regression model.

Estimate (β)	Left				Right			
	FA	MD	RD	AD	FA	MD	RD	AD
TD								
Age in months	-0.001	0.001	0.001	0.001*	-0.001	0.001*	0.001*	0.001
Females (n=19)	0.011	−0.004	−0.009	0.006	0.009	0.050	0.036	0.079
Left-handed (n=4)	0.067*	−0.104*	−0.134*	−0.043	0.062**	−0.051	−0.090	0.028
22q11.2DS								
Age in months	−0.001	−0.001	−0.001	−0.001	0.001	−0.001	−0.001	−0.002
Females (n=23)	−0.016	−0.027	−0.003	−0.073	−0.018	−0.014	0.007	−0.055
Left-handed (n=9)	0.027	0.086*	0.039	0.179**	0.029	0.053	0.011	0.137*

Note: TD, typically developing children. Some values were set to 0 because they were used as the reference for modeling. They are gender = male, handedness = right-handed. In addition, age in months was centered at 80 months.

* *p*-Value < 0.05.
** *p*-Value < 0.01.

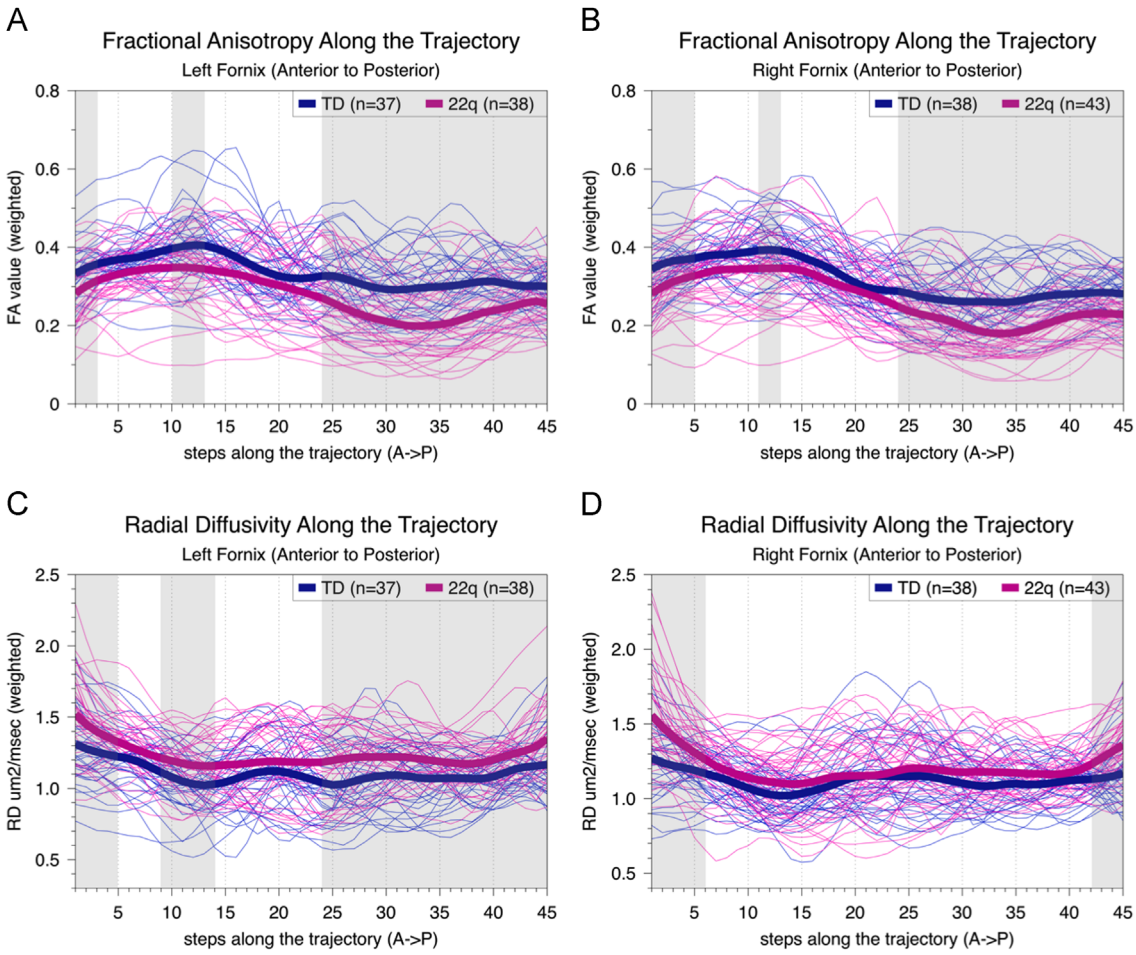

Fig. 2. FA and RD values vary along the trajectory and significantly differ between groups especially at the posterior area. Each single line represents segments of diffusion properties along the body of fornix from anterior to posterior in each individual brain in both TD group (blue) and the 22q11.2DS group (pink). The two bold lines represent the group means at each segment. Segments with a significant group difference after FDR correction are highlighted in grey.

Table 4
The volume of the hippocampal formation and regression coefficients with fornix diffusivity properties in each group after controlling for the effect of age and gender.

	Hippocampal formation volume (mm^3)		Estimate (β)					
	n	Mean (S.D.)	Fornix FA			Fornix RD		
			Across the tract	anterior	posterior	Across the tract	anterior	posterior
TD								
Left	38	2.27 (0.34)	0.019	0.016	−0.010	−0.067	−0.055	0.002
Right	38	2.48 (0.42)	0.021	0.066*	−0.003	−0.025	−0.147	−0.023
22q11.2DS								
Left	37	1.77 (0.47)	0.021	0.032	0.041	−0.042	−0.160	−0.011
Right	42	1.99 (0.53)	0.054**	0.046*	0.060**	−0.067*	−0.136*	−0.123*

Note: TD, typically developing children. Linear regression models were used to access the correlation between fornix diffusivity and the volume of the hippocampal formation, with age and gender entered as covariates.

* p-Value < 0.05.
** p-Value < 0.01.

midline structural anomalies and fornix characteristics. In rodents, cytotoxic lesions in anterior thalamic nuclei or fornix are related to spatial working memory impairments, but not object recognition (Aggleton et al., 1995), adding evidence to the role of hippocampal-anterior thalamic connections in visuospatial cognition. However, we need to bear in mind that measures of water anisotropy and radial diffusivity in a magnetic field provides only an indirectly and confounded, gross picture of the brain organization, especially in the subcortical area surrounded by CSF. Thus, the question of why fornix integrity is disrupted more in these specific regions is still open, and beyond the capability of current DTI tractography to answer.

In this study, there was a small subset containing eight children with 22q11.2DS, for whom ConTrack was unable to reconstruct a fornix fiber tract between the anterior and posterior seeds. Although we limited excessive motion through training, one possible reason is that image artifacts from subtle patient motion reduced the accuracy

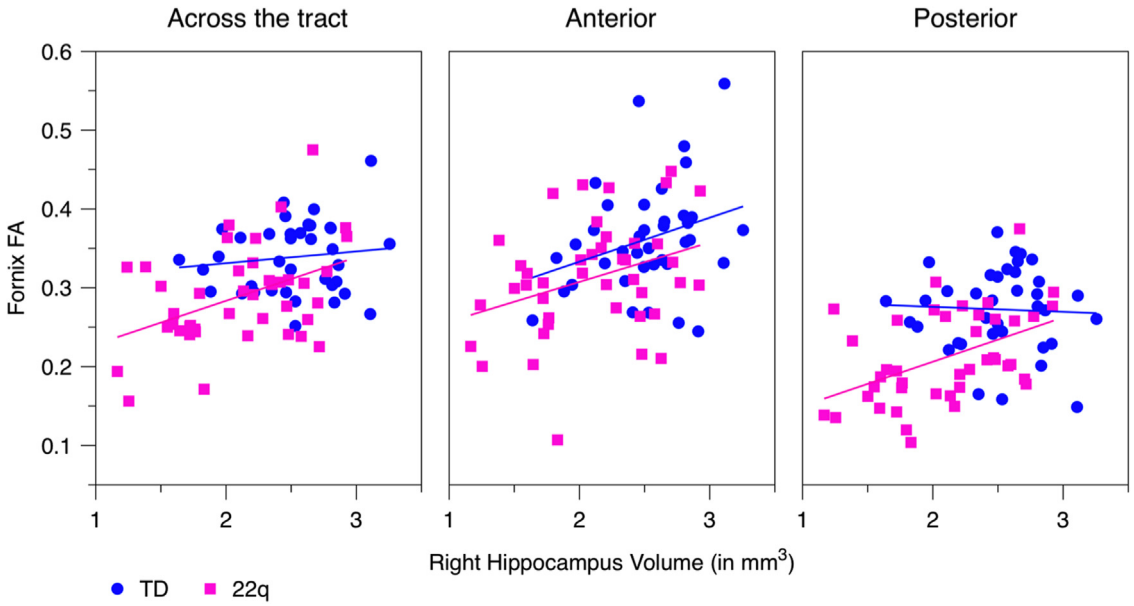

Fig. 3. Scatter plot of the fornix fractional anisotropy (FA) value and the volume of hippocampal formation in the right hemisphere in the 22q11.2DS group (pink) and the TD group (blue).

and precision of the acquired DT-image data. Another possible reason is that the characteristic midline anatomical anomalies commonly detected in these brains were in some way related to the development of an abnormal fornix tract. Three of these eight brains were ones that contained enlarged CSP ($n=2$) and/or dilated lateral ventricles ($n=1$), while another showed atypical asymmetric fornix distortion. Thus, the grossly atypical fornix itself in these brains is the most likely explanation for ConTrack failing to meet the confidence threshold to reconstruct the fibers after 100,000 permutations. As a probabilistic tracking algorithm, ConTrack identifies the most likely pathways between two regions by first sampling a broad range of potential pathways, then scoring the pathway's anatomical validity (Sherbondy et al., 2008a). It expands the pathway search space, thereby exploring alternative connections without *a priori* assumptions. Therefore, although it better accounts for data uncertainty and unresolved features like crossing fibers, it also increases the possibility of incorporating neighboring fibers when the diffusion directional signal is too low relative to the amount of noise to allow for precise tracking. This is particularly true in more anatomically atypical brains, which are commonly found in individuals with 22q11.2DS. One final possibility for this difficulty is that the hippocampus itself in these brains was sufficiently abnormal to generate a detectable fornix. Notably, three of these eight brains contain an abnormally small hippocampal formation in the left hemisphere, with volumes ranging from 1.08 mm^3 to 1.58 mm^3, much lower than the 22q11.2DS group mean (1.77 mm^3). Clearly an abnormally small hippocampus, as is often reported in individuals with 22q11.2DS, could alter the integrity of the fornix to a point at which the fibers within the fornix could not be identified.

Similar to our findings, lower FA and higher RD in the body of the fornix have been consistently reported in patients with schizophrenia (Fitzsimmons et al., 2009; Luck et al., 2010; Qiu et al., 2010; Abdul-Rahman et al., 2011), despite differences in the applied diffusion tensor based tracking technique. Abdul-Rahman and colleagues found that FA reduction in the fornix was correlated with greater severity of psychotic symptoms (Abdul-Rahman et al., 2011), which they interpreted as a result of underlying demyelination, axonal damage or a combination of both processes, and they suggested that atypical hippocampal connectivity circuits might account for the cognitive impairments in patients with schizophrenia. Even though the relationship between actual psychotic symptomatology and the 22q11.2DS remains unclear, the similarity in diffusion patterns may suggest a biological basis of spatial cognitive impairments and other schizophrenia-related risk factors in this population.

We acknowledge several limitations in this study. Firstly, fornix tractography was performed using diffusion-weighted images obtained from a standard 12-direction DTI pulse sequence without cerebrospinal fluid (CSF) suppression. Partial volume from the rapid, isotropically diffusing CSF (Concha et al., 2005) may adversely affect the absolute diffusion characteristics of the fornix. Therefore a fluid-attenuated inversion recovery (FLAIR) DTI sequence (Hajnal et al., 1992) may be an optimal solution for the subcortical tractography. In this study, the possible partial volume effect was minimized by seeding ROIs on the perpendicular slices of the fornix (Kuroki et al., 2006) and tracking using a probabilistic algorithm, as it evaluates the likelihoods connecting two regions in an expanding pathway search space (Sherbondy et al., 2008a). Even though, the fornix tract was found to be significantly shorter in the 22q11.2DS group in the original tractography step, this result could possibly arise from a combination of a white matter structural deficit and/or an image artifact, since the fornix tract might be “non-trackable” in the posterior part where it bends most because of partial volume effect. Second, the ROIs were defined on the DTI co-registered T1 images rather than DT images, due to their limited resolution. Seeding on a high-resolution structural T1 ensured the anatomical accuracy, but also introduced the possibility of small misregistration errors. Indeed, the DTI-T1 registration was difficult in children brains, particularly in an atypical population like 22q11.2DS with anatomical anomalies. We minimized the misregistration confounds by seeding the ROIs in a conservative manner with respect to an individual's brain anatomy. Third, we did not measure medication effects in this study because none of the medications used by children in the study was taken by more than just a few children in each case (see Supplementary material), which would have made any systematic study of medication effects impossible. The effect of medications on white matter integrity and connectivity is worthy of inviting further investigation with larger samples.

In conclusion, using diffusion tensor based tractography, a less organized fornix with significantly lower FA and higher RD was found in children with 22q11.2DS as a group, yet variable, compared with age-matched typically developing children. This fornix integrity disruption was detected especially prominent in the posterior aspect where the fornix projects from the hippocampus.

Together with the anomalies in hippocampal formation volumes, our findings add neuroanatomical evidence of disrupted hippocampal connectivity in children with 22q11.2DS, which may help to further understand the biological basis of spatial cognitive impairments and other schizophrenia-related risk factors in this population.

Acknowledgements

This work was supported by a National Institutes of Health (Grant R01HD042974 to T.J.S. and Grant AG030514 to O.T.C).

Appendix A. Supplementary materials

Supplementary data associated with this article can be found in the online version at http://dx.doi.org/10.1016/j.pscychresns.2015.02.002.

References

Abdul-Rahman, M.F., Qiu, A., Sim, K., 2011. Regionally specific white matter disruptions of fornix and cingulum in schizophrenia. PloS One 6, e18652.
Aggleton, J.P., Neave, N., Nagle, S., Hunt, P.R., 1995. A comparison of the effects of anterior thalamic, mamillary body and fornix lesions on reinforced spatial alternation. Behavioural Brain Research 68, 91–101.
Akers, D., 2006. CINCH: a cooperatively designed marking interface for 3D pathway selection. Paper presented at the User Interface Software and Technology (UIST).
Angkustsiri, K., Leckliter, I.N., Tartaglia, N., Beaton, E.A., Enriquez, J., Simon, T.J., 2012. An examination of the relationship of anxiety and intelligence to adaptive functioning in children with chromosome 22q11.2 deletion syndrome. Journal of Developmental and Behavioral Pediatrics 33, 713–720.
Antshel, K., Conchelos, J., Lanzetta, G., Fremont, W., Kates, W., 2005. Behavior and corpus callosum morphology relationships in velocardiofacial syndrome (22q11.2 deletion syndrome). Psychiatry Research: Neuroimaging 138, 235–245.
Arnold, P.D., Siegel-Bartelt, J., Cytrynbaum, C., Teshima, I., Schachar, R., 2001. Velo-cardio-facial syndrome: Implications of microdeletion 22q11 for schizophrenia and mood disorders. American Journal of Medical Genetics 105, 354–362.
Ashburner, J., Friston, K.J., 2005. Unified segmentation. Neuroimage 26, 839–851.
Avants, B.B., Tustinson, N.J., Wu, J., Cook, P.A., Gee, J.C., 2011. An open source multivariate framework for n-tissue segmentation with evaluation on public data. Neuroinformatics 9, 381–400.
Baker, K.D., Skuse, D.H., 2005. Adolescents and young adults with 22q11 deletion syndrome: psychopathology in an at-risk group. British Journal of Psychiatry 186, 115–120.
Barnea-Goraly, N., Eliez, S., Menon, V., Bammer, R., Reiss, A.L., 2005. Arithmetic ability and parietal alterations: a diffusion tensor imaging study in velocardiofacial syndrome. Cognitive Brain Research 25, 735–740.
Barnea-Goraly, N., Menon, V., Krasnow, B., Ko, A., Reiss, A., Eliez, S., 2003. Investigation of white matter structure in velocardiofacial syndrome: a diffusion tensor imaging study. American Journal of Psychiatry 160, 1863–1869.
Basser, P.J., Pierpaoli, C., 1996. Microstructural and physiological features of tissues elucidated by quantitative-diffusion-tensor MRI. Journal of Magnetic Resonance, Series B 111, 209–219.
Bassett, A.S., Chow, E.W., 1999. 22q11 deletion syndrome: a genetic subtype of schizophrenia. Biological Psychiatry 46, 882–891.
Bearden, C.E., van Erp, T.G.M., Dutton, R.A., Lee, A.D., Simon, T.J., Cannon, T.D., Emanuel, B.S., McDonald-McGinn, D., Zackai, E.H., Thompson, P.M., 2009. Alterations in midline cortical thickness and gyrification patterns mapped in children with 22q11.2 deletions. Cerebral Cortex 19, 115–126.
Bearden, C.E., van Erp, T.G.M., Dutton, R.A., Tran, H., Zimmermann, L., Sun, D., Geaga, J.A., Simon, T.J., Glahn, D.C., Cannon, T.D., Emanuel, B.S., Toga, A.W., Thompson, P.M., 2007. Mapping cortical thickness in children with 22q11.2 deletions. Cerebral Cortex 17, 1889–1898.
Bearden, C.E., Woodin, M.F., Wang, P.P., Moss, E., McDonald-McGinn, D., Zackai, E., Emannuel, B., Cannon, T.D., 2001. The neurocognitive phenotype of the 22q11.2 deletion syndrome: selective deficit in visual-spatial memory. Journal of Clinical Experimental Neuropsychology 23, 447–464.
Beaton, E.A., Qin, Y., Nguyen, V., Johnson, J., Pinter, J.D., Simon, T.J., 2010. Increased incidence and size of cavum septum pellucidum in children with chromosome 22q11.2 deletion syndrome. Psychiatry Research: Neuroimaging 181, 108–113.
Bish, J.P., Chiodo, R., Mattei, V., Simon, T.J., 2007. Domain specific attentional impairments in children with chromosome 22q11.2 deletion syndrome. Brain and Cognition 64, 265–273.
Bish, J.P., Nguyen, V., Ding, L., Ferrante, S., Simon, T.J., 2004. Thalamic reductions in children with chromosome 22q11.2 deletion syndrome. Neuroreport 15, 1413–1415.
Bishop, S.J., 2009. Trait anxiety and impoverished prefrontal control of attention. Nature Neuroscience 12, 92–98.
Botto, L.D., May, K., Fernhoff, P.M., Correa, A., Coleman, K., Rasmussen, S.A., Merritt, R.K., O'Leary, L.A., Wong, L.-Y., Elixson, E.M., Mahle, W.T., Campbell, R.M., 2003. A population-based study of the 22q11.2 deletion: phenotype, incidence, and contribution to major birth defects in the population. Pediatrics 112, 101–107.
Campbell, L.E., Daly, E., Toal, F., Stevens, A., Azuma, R., Catani, M., Ng, V., van Amelsvoort, T., Chitnis, X., Cutter, W., Murphy, D.G.M., Murphy, K.C., 2006. Brain and behaviour in children with 22q11.2 deletion syndrome: a volumetric and voxel-based morphometry MRI study. Brain 129, 1218–1228.
Carey, A.H., Kelly, D., Halford, S., Wadey, R., Wilson, D., Goodship, J., Burn, J., Paul, T., Sharkey, A., Dumanski, J., 1992. Molecular genetic study of the frequency of monosomy 22q11 in DiGeorge syndrome. American Journal of Human Genetics 51, 964–970.
Chang, L.-C., Jones, D.K., Pierpaoli, C., 2005. RESTORE: robust estimation of tensors by outlier rejection. Magnetic Resonance in Medicine 53, 1088–1095.
Concha, L., Gross, D.W., Beaulieu, C., 2005. Diffusion tensor tractography of the limbic system. AJNR American Journal of Neuroradiology 26, 2267–2274.
Debbané, M., Schaer, M., Farhoumand, R., Glaser, B., Eliez, S., 2006. Hippocampal volume reduction in 22q11.2 deletion syndrome. Neuropsychologia 44, 2360–2365.
Deboer, T., Wu, Z., Lee, A., Simon, T.J., 2007. Hippocampal volume reduction in children with chromosome 22q11.2 deletion syndrome is associated with cognitive impairment. Behavioral and Brain Functions 3, 54.
Driscoll, D.A., Budarf, M.L., Emanuel, B.S., 1992. A genetic etiology for DiGeorge syndrome: consistent deletions and microdeletions of 22q11. American Journal of Human Genetics 50, 924–933.
Eliez, S., Schmitt, J., White, C.D., Reiss, A.L., 2000. Children and adolescents with velocardiofacial syndrome: a volumetric MRI study. American Journal of Psychiatry 157, 409–415.
Fitzsimmons, J., Kubicki, M., Smith, K., Bushell, G., Estepar, R.S.J., Westin, C.-F., Nestor, P.G., Niznikiewicz, M.A., Kikinis, R., McCarley, R.W., Shenton, M.E., 2009. Diffusion tractography of the fornix in schizophrenia. Schizophrenia Research 107, 39–46.
Flahault, A., Schaer, M., Ottet, M.-C., Debbané, M., Eliez, S., 2012. Hippocampal volume reduction in chromosome 22q11.2 deletion syndrome (22q11.2DS): a longitudinal study of morphometry and symptomatology. Psychiatry Research: Neuroimaging 203, 1–5.
Gray, J.A., McNaughton, N., 2000. The Neuropsychology of Anxiety: An Enquiry into the Functions of the Septo-Hippocampal System, 2nd ed. Oxford University Press, Oxford.
Green, T., Gothelf, D., Glaser, B., Debbane, M., Frisch, A., Kotler, M., Weizman, A., Eliez, S., 2009. Psychiatric disorders and intellectual functioning throughout development in velocardiofacial (22q11.2 deletion) syndrome. Journal of the American Academy of Child and Adolescent Psychiatry 48, 1060–1068.
Hajnal, J.V., Bryant, D.J., Kasuboski, L., Pattany, P.M., De Coene, B., Lewis, P.D., Pennock, J.M., Oatridge, A., Young, I.R., Bydder, G.M., 1992. Use of fluid attenuated inversion recovery (FLAIR) pulse sequences in MRI of the brain. Journal of Computer Assisted Tomography 16, 841–844.
Hunsaker, M.R., Amaral, D.G., 2014. A semi-automated pipeline for the segmentation of rhesus macaque hippocampus: validation across a wide age range. PloS One 9, e89456.
Karayiorgou, M., Simon, T.J., Gogos, J.A., 2010. 22q11.2 microdeletions: linking DNA structural variation to brain dysfunction and schizophrenia. Nature Reviews. Neuroscience 11, 402–416.
Kates, W.R., Burnette, C.P., Jabs, E.W., Rutberg, J., Murphy, A.M., Grados, M., Geraghty, M., Kaufmann, W.E., Pearlson, G.D., 2001. Regional cortical white matter reductions in velocardiofacial syndrome: a volumetric MRI analysis. Biological Psychiatry 49, 677–684.
Kates, W.R., Antshel, K.M., Faraone, S.V., Fremont, W.P., Higgins, A.M., Shprintzen, R.J., Botti, J.-A., Kelchner, L., McCarthy, C., 2011. Neuroanatomic predictors to prodromal psychosis in velocardiofacial syndrome (22q11.2 deletion syndrome): a longitudinal study. Biological Psychiatry 69, 945–952.
Kates, W.R., Burnette, C.P., Bessette, B.A., Folley, B.S., Strunge, L., Jabs, E.W., Pearlson, G.D., 2004. Frontal and caudate alterations in velocardiofacial syndrome (deletion at chromosome 22q11.2). Journal of Child Neurology 19, 337–342.
Kates, W.R., Miller, A.M., Abdulsabur, N., Antshel, K.M., Conchelos, J., Fremont, W., Roizen, N., 2006. Temporal lobe anatomy and psychiatric symptoms in velocardiofacial syndrome (22q11.2 deletion syndrome). Journal of American Academy of Child and Adolescent Psychiatry 45, 587–595.
Kirkpatrick, J.A., DiGeorge, A.M., 1968. Congenital absence of the thymus. American Journal of Roentgenology, Radium Therapy, and Nuclear Medicine 103, 32–37.
Krug, M.K., Carter, C.S., 2010. Adding fear to conflict: a general purpose cognitive control network is modulated by trait anxiety. Cognitive, Affective and Behavioral Neuroscience 10, 357–371.
Kuroki, N., Kubicki, M., Nestor, P.G., Salisbury, D.F., Park, H.-J., Levitt, J.J., Woolston, S., Frumin, M., Niznikiewicz, M., Westin, C.-F., Maier, S.E., McCarley, R.W., Shenton, M.E., 2006. Fornix integrity and hippocampal volume in male schizophrenic patients. Biological Psychiatry 60, 22–31.
Lau, J.Y.F., Lissek, S., Nelson, E.E., Lee, Y., Roberson-Nay, R., Poeth, K., Jenness, J., Ernst, M., Grillon, C., Pine, D.S., 2008. Fear conditioning in adolescents with anxiety disorders: results from a novel experimental paradigm. Journal of American Academy of Child and Adolescent Psychiatry 47, 94–102.

LeDoux, J.E., 2000. Emotion circuits in the brain. Annual Review of Neuroscience 23, 155–184.
Lee, D.Y., Fletcher, E., Carmichael, O.T., Singh, B., Mungas, D., Reed, B., Martinez, O., Buonocore, M.H., Persianinova, M., Decarli, C., 2012. Sub-regional hippocampal injury is associated with fornix degeneration in Alzheimer's disease. Frontiers in Aging Neuroscience 4, 1–10.
Lissek, S., Levenson, J., Biggs, A.L., Johnson, L.L., Ameli, R., Pine, D.S., Grillon, C., 2008. Elevated fear conditioning to socially relevant unconditioned stimuli in social anxiety disorder. American Journal of Psychiatry 165, 124–132.
Luck, D., Malla, A.K., Joober, R., Lepage, M., 2010. Disrupted integrity of the fornix in first-episode schizophrenia. Schizophria Research 119, 61–64.
Machado, A.M.C., Simon, T.J., Nguyen, V., McDonald-McGinn, D.M., Zackai, E.H., Gee, J.C., 2007. Corpus callosum morphology and ventricular size in chromosome 22q11.2 deletion syndrome. Brain Research 1131, 197–210.
Metzler-Baddeley, C., Jones, D.K., Belaroussi, B., Aggleton, J.P., O'Sullivan, M.J., 2011. Frontotemporal connections in episodic memory and aging: a diffusion MRI tractography study. Journal of Neuroscience 31, 13236–13245.
Moss, E.M., Batshaw, M.L., Solot, C.B., Gerdes, M., McDonald-McGinn, D.M., Driscoll, D.A., Emanuel, B.S., Zackai, E.H., Wang, P.P., 1999. Psychoeducational profile of the 22q11.2 microdeletion: a complex pattern. Journal of Pediatrics 134, 193–198.
Murphy, K.C., Jones, L.A., Owen, M.J., 1999. High rates of schizophrenia in adults with velo-cardio-facial syndrome. Archives of General Psychiatry 56, 940–945.
Olsen, R.K., Moses, S.N., Riggs, L., Ryan, J.D., 2012. The hippocampus supports multiple cognitive processes through relational binding and comparison. Frontiers in Human Neuroscience 6, 1–13.
Pérez-Edgar, K., Fox, N.A., 2007. Temperamental contributions to children's performance in an emotion-word processing task: a behavioral and electrophysiological study. Brain and Cognition 65, 22–35.
Pérez-Edgar, K., Reeb-Sutherland, B.C., McDermott, J.M., White, L.K., Henderson, H.A., Degnan, K.A., Hane, A.A., Pine, D.S., Fox, N.A., 2011. Attention biases to threat link behavioral inhibition to social withdrawal over time in very young children. Journal of Abnormal Child Psychology 39, 885–895.
Pluta, J., Avants, B.B., Glynn, S., Awate, S., Gee, J.C., Detre, J.A., 2009. Appearance and incomplete label matching for diffeomorphic template based hippocampus segmentation. Hippocampus 19, 565–571.
Qiu, A., Tuan, T.A., Woon, P.S., Abdul-Rahman, M.F., Graham, S., Sim, K., 2010. Hippocampal-cortical structural connectivity disruptions in schizophrenia: an integrated perspective from hippocampal shape, cortical thickness, and integrity of white matter bundles. Neuroimage 52, 1181–1189.
Radoeva, P.D., Coman, I.L., Antshel, K.M., Fremont, W., McCarthy, C.S., Kotkar, A., Wang, D., Shprintzen, R.J., Kates, W.R., 2012. Atlas-based white matter analysis in individuals with velo-cardio-facial syndrome (22q11.2 deletion syndrome) and unaffected siblings. Behavioral and Brain Functions 8, 38–48.
Rohde, G.K., Barnett, A.S., Basser, P.J., Marenco, S., Pierpaoli, C., 2004. Comprehensive approach for correction of motion and distortion in diffusion-weighted MRI. Magnetic Resonance in Medicine 51, 103–114.
Roy, A.K., Vasa, R.A., Bruck, M., Mogg, K., Bradley, B.P., Sweeney, M., Bergman, R.L., McClure-Tone, E.B., Pine, D.S., Team, C., 2008. Attention bias toward threat in pediatric anxiety disorders. Journal of American Academy of Child and Adolescent Psychiatry 47, 1189–1196.
Schaer, M., Glaser, B., Cuadra, M.B., Debbane, M., Thiran, J.-P., Eliez, S., 2009. Congenital heart disease affects local gyrification in 22q11.2 deletion syndrome. Develomental Medicine and Child Neurology 51, 746–753.
Schaer, M., Schmitt, J.E., Glaser, B., Lazeyras, F., Delavelle, J., Eliez, S., 2006. Abnormal patterns of cortical gyrification in velo-cardio-facial syndrome (deletion 22q11.2): an MRI study. Psychiatry Research: Neuroimaging 146, 1–11.
Schumann, C.M., Hamstra, J., Goodlin-Jones, B.L., Kwon, H., Reiss, A.L., Amaral, D.G., 2007. Hippocampal size positively correlates with verbal IQ in male children. Hippocampus 17, 486–493.
Shashi, V., Muddasani, S., Santos, C.C., Berry, M.N., Kwapil, T.R., Lewandowski, E., Keshavan, M.S., 2004. Abnormalities of the corpus callosum in nonpsychotic children with chromosome 22q11 deletion syndrome. Neuroimage 21, 1399–1406.
Shashi, V., Veerapandiyan, A., Keshavan, M.S., Zapadka, M., Schoch, K., Kwapil, T.R., Hooper, S.R., Stanley, J.A., 2012. Altered development of the dorsolateral prefrontal cortex in chromosome 22q11.2 deletion syndrome: an in vivo proton spectroscopy study. Biological Psychiatry 72, 684–691.
Shenton, M.E., Dickey, C.C., Frumin, M., McCarley, R.W., 2001. A review of MRI findings in schizophrenia. Schizophria Research 49, 1–52.
Sherbondy, A.J., Dougherty, R.F., Ben-Shachar, M., Napel, S., Wandell, B.A., 2008a. ConTrack: finding the most likely pathways between brain regions using diffusion tractography. Journal of Vision 8, 1–16.
Sherbondy, A.J., Dougherty, R.F., Napel, S., Wandell, B.A., 2008b. Identifying the human optic radiation using diffusion imaging and fiber tractography. Journal of Vision 8, 1–11.
Shprintzen, R.J., 2008. Velo-cardio-facial syndrome: 30 years of study. Developmental Disabilities Research Reviews 14, 3–10.
Shprintzen, R.J., Goldberg, R.B., Lewin, M.L., Sidoti, E.J., Berkman, M.D., Argamaso, R.V., Young, D., 1978. A new syndrome involving cleft palate, cardiac anomalies, typical facies, and learning disabilities: velo-cardio-facial syndrome. Cleft Palate Journal 15, 56–62.
Simon, T.J., Bearden, C.E., Mc-Ginn, D.M., Zackai, E., 2005a. Visuospatial and numerical cognitive deficits in children with chromosome 22q11.2 deletion syndrome. Cortex 41, 145–155.
Simon, T.J., Bish, J.P., Bearden, C.E., Ding, L., Ferrante, S., Nguyen, V., Gee, J.C., McDonald-McGinn, D.M., Zackai, E.H., Emanuel, B.S., 2005b. A multilevel analysis of cognitive dysfunction and psychopathology associated with chromosome 22q11.2 deletion syndrome in children. Developmental Psychopathology 17, 753–784.
Simon, T.J., Ding, L., Bish, J.P., McDonald-McGinn, D.M., Zackai, E.H., Gee, J., 2005c. Volumetric, connective, and morphologic changes in the brains of children with chromosome 22q11.2 deletion syndrome: an integrative study. Neuroimage 25, 169–180.
Simon, T.J., Takarae, Y., DeBoer, T., McDonald-McGinn, D.M., Zackai, E.H., Ross, J.L., 2008a. Overlapping numerical cognition impairments in children with chromosome 22q11.2 deletion or Turner syndromes. Neuropsychologia 46, 82–94.
Simon, T.J., Wu, Z., Avants, B., Zhang, H., Gee, J.C., Stebbins, G.T., 2008b. Atypical cortical connectivity and visuospatial cognitive impairments are related in children with chromosome 22q11.2 deletion syndrome. Behavioral and Brain Functions 4, 4–25.
Sled, J.G., Zijdenbos, A.P., Evans, A.C., 1998. A nonparametric method for automatic correction of intensity nonuniformity in MRI data. IEEE Translational on Medical Imaging 17, 87–97.
Srivastava, S., Buonocore, M.H., Simon, T.J., 2011. Atypical developmental trajectory of functionally significant cortical areas in children with chromosome 22q11.2 deletion syndrome. Human Brain Mapping 33, 213–223.
Stoddard, J., Niendam, T., Hendren, R., Carter, C., Simon, T.J., 2010. Attenuated positive symptoms of psychosis in adolescents with chromosome 22q11.2 deletion syndrome. Schizophrenia Research 118, 118–121.
Sundram, F., Campbell, L.E., Azuma, R., Daly, E., Bloemen, O.J.N., Barker, G.J., Chitnis, X., Jones, D.K., Amelsvoort, T.V., Murphy, K.C., Murphy, D.G.M., 2010. White matter microstructure in 22q11 deletion syndrome: a pilot diffusion tensor imaging and voxel-based morphometry study of children and adolescents. Journal of Neurodevelopmental Disorders 2, 77–92.
Swillen, A., Devriendt, K., Legius, E., Prinzie, P., Vogels, A., Ghesquière, P., Fryns, J.P., 1999a. The behavioural phenotype in velo-cardio-facial syndrome (VCFS): from infancy to adolescence. Genetic Counseling 10, 79–88.
Swillen, A., Vandeputte, L., Cracco, J., Maes, B., Ghesquière, P., Devriendt, K., Fryns, J.P., 1999b. Neuropsychological, learning and psychosocial profile of primary school aged children with the velo-cardio-facial syndrome (22q11 deletion): evidence for a nonverbal learning disability? Child Neuropsychology 5, 230–241.
Tustison, N.J., Avants, B.B., Cook, P.A., Zheng, Y., Egan, A., Yushkevich, P.A., Gee, J.C., 2010. N4ITK: improved N3 bias correction. IEEE Transactions on Medical Imaging 29, 1310–1320.
Wang, P.P., Woodin, M.F., Kreps-Falk, R., Moss, E.M., 2000. Research on behavioral phenotypes: velocardiofacial syndrome (deletion 22q11.2). Developmental Medicine and Child Neurology 42, 422–427.
Yeatman, J.D., Dougherty, R.F., Myall, N.J., Wandell, B.A., Feldman, H.M., 2012. Tract profiles of white matter properties: automating fiber-tract quantification. PLoS One 7, e49790.
Yeatman, J.D., Dougherty, R.F., Rykhlevskaia, E., Sherbondy, A.J., Deutsch, G.K., Wandell, B.A., Ben-Shachar, M., 2011. Anatomical properties of the arcuate fasciculus predict phonological and reading skills in children. Journal of Cognitive Neuroscience 23, 3304–3317.